

## TERZAGHI'S EFFECTIVE STRESS PRINCIPLE AND HYDROLOGICAL DEFORMATION OF KARST MASSIFS DETECTED BY GNSS AND INSAR

GUIDO LEONE<sup>(\*)</sup>, MICHELE GINOLFI<sup>(\*)</sup>, LIBERA ESPOSITO<sup>(\*)</sup> & FRANCESCO FIORILLO<sup>(\*)</sup>

<sup>(\*)</sup>University of Sannio - Department of Sciences and Technologies - Benevento, Italy  
Corresponding author: guleone@unisannio.it

### EXTENDED ABSTRACT

I massicci carsici carbonatici della catena appenninica rappresentano importanti acquiferi che alimentano potenti sorgenti basali, per le quali sono disponibili serie temperali giornaliere delle portate. In alcuni casi, i predetti massicci sono monitorati da stazioni GNSS (*Global Navigation Satellite Systems*) permanenti, le quali forniscono registrazioni continue dello spostamento del suolo al sito di misura. L'analisi di questi dati ha rilevato una chiara componente idrologica che interessa gli spostamenti nel piano orizzontale. Al fine di spiegare tale componente, vari studi hanno applicato specifici approcci di modellazioni, i quali assumono che le fluttuazioni dei carichi idraulici, dovute al processo di ricarica-svuotamento degli acquiferi, causerebbero l'apertura e la chiusura delle fratture dell'ammasso roccioso, a seguito delle variazioni della pressione dell'acqua contenuta al loro interno. Tali modelli, tuttavia, attribuiscono la deformazione dei massicci carsici esclusivamente all'idrodinamica delle fratture principali, trascurando il ruolo della pressione di poro esercitata dall'acqua nella zona satura. Difatti, gli acquiferi carsici vengono generalmente schematizzati come mezzi aventi tre componenti di porosità, cioè come mezzi dove l'acqua riempie (i) vuoti di grandi dimensioni e condotti, (ii) fratture, nonché pori e fessure (matrice). La risorsa idrica sotterranea principale è contenuta nella zona satura dell'acquifero, che comprende sia la rete carsica di fratture e condotti, contraddistinta da una elevata permeabilità, sia la matrice, contraddistinta da una ridotta permeabilità e una grande capacità di immagazzinamento. Inoltre, scambi di acqua si verificano tra la rete carsica e la matrice. In generale, ampie oscillazioni della tavola d'acqua caratterizzano gli acquiferi carsici dell'Appennino, le quali sono favorite dalle abbondanti precipitazioni tipiche di questo settore del bacino Mediterraneo. Le fasi di basso e alto stazionamento della tavola d'acqua sono associate a variazioni della pressione di poro fino a centinaia di kPa in profondità. Queste ultime interessano principalmente la zona satura e la zona epifreatica dell'acquifero e, pertanto, causano variazioni nello stato tensionale di un ampio volume roccioso, per il principio degli sforzi efficaci. Questo studio tratta del meccanismo di deformazione idrologica dei massicci carsici e descrive le equazioni che legano detta deformazione alle variazioni dei livelli di falda. Il presente lavoro discute il caso studio del massiccio del Matese (Italia meridionale) e mostra che le serie temporali GNSS acquisite in quest'area, analogamente a quanto osservato in altre aree carsiche dell'Appennino, contengono una componente idrologica. In particolare, esiste una chiara correlazione tra le variazioni stagionali e a lungo termine delle portate sorgive e gli spostamenti del suolo nel piano orizzontale (opportunamente processati). Viceversa, non è stata osservata una chiara componente idrologica negli spostamenti nel piano verticale misurati ai singoli siti GNSS. Tuttavia, dall'analisi di dati InSAR (*Interferometric Synthetic Aperture Radar*) è emersa una correlazione positiva tra le portate sorgive e lo spostamento verticale del suolo misurato nel settore occidentale del massiccio. Questo studio illustra una nuova spiegazione fisica al fenomeno idrologico osservato, basata sul principio degli sforzi efficaci di Terzaghi e l'elasticità lineare classica. In particolare, è stata adottata la formulazione degli sforzi efficaci proposta da Skempton, la quale estende il principio di Terzaghi alle rocce sature. La causa della deformazione idrologica osservata è innanzitutto legata alle variazioni della pressione di poro nella zona satura dell'acquifero, associate all'innalzamento e all'abbassamento della tavola d'acqua. Le equazioni proposte sono state derivate assumendo due distinte condizioni dell'acquifero carsico: nel primo caso (*unconstrained-strain*), l'acquifero è libero di espandersi lateralmente e lo *strain* idrologico dipende dalle proprietà elastiche generali dell'ammasso roccioso e dal coefficiente di spinta a riposo  $K_0$ ; nel secondo caso (*constrained-strain*), l'acquifero è limitato lateralmente da un *aquitard* e lo *strain* dipende anche dalle proprietà elastiche e dalle dimensioni di quest'ultimo. Lo *strain* risultante, pertanto, è una frazione dell'*unconstrained-strain*. La deformazione idrologica osservata può essere comparata all'espansione termica dei solidi, la cui entità dipende dalle caratteristiche fisiche e geometriche del materiale e dall'incremento di temperatura. In maniera simile, la deformazione idrologica è causata dalla variazione della pressione di poro e investe l'intero volume saturo dell'acquifero. Gli spostamenti del suolo registrati alle stazioni GNSS dipendono anche dalla loro ubicazione, poiché essi sono il risultato della deformazione idrologica accumulata attraverso l'acquifero.

## ABSTRACT

Previous studies have shown that carbonate massifs of the Apennine chain (Italy) undergo deformation in response to groundwater level variations occurring in the saturated zone of karst aquifers. This study focuses on the Matese massif, hosting one of the main karst aquifers of the central-southern Apennine. Our analyses revealed a hydrological component in the time series of the horizontal and vertical ground displacements measured by GNSS (Global Navigation Satellite Systems) and InSAR (Interferometric Synthetic Aperture Radar). In particular, contraction and dilatation phases of the karst massif appear associated with the lowering and rising of the groundwater levels, respectively. Various authors have explained this phenomenon by the widening and closing of sub-vertical water-filled fractures dissecting the rock mass due to varying hydraulic heads, neglecting the role of the effective stress state acting in the aquifer saturated zone. We present new equations explaining the observed deformational phenomenon in its generality, which are based on Terzaghi's effective stress principle (Skempton's generalization) and linear elasticity. The study shows that hydrological deformation of karst massifs is similar to the thermal expansion of solids. In the first case, the deformation is primarily due to pore water pressure variations occurring in the aquifer saturated zone, which are associated with water table oscillations, and is controlled by the elastic properties of the rock mass and the coefficient of earth pressure at rest,  $K_0$ .

**KEYWORDS:** hydrological deformation, GNSS, InSAR, karst aquifer, pore water pressure, coefficient of earth pressure at rest, Terzaghi's principle, poroelasticity

## INTRODUCTION

GNSS (Global Navigation Satellite Systems) and InSAR (Interferometric Synthetic Aperture Radar) studies have shown that changes in the hydrological stage of aquifers lead to the deformation of the Earth's crust (BELL *et alii*, 2002; RIEL *et alii*, 2018; SILVERI *et alii*, 2019; WHITE *et alii*, 2022). The hydrological ground motion is superposed on the displacement associated with other processes, including tectonic motion, atmospheric pressure loading, and tidal and non-tidal fluctuations in the ocean (BAWDEN *et alii*, 2001; VAN DAM *et alii*, 2001).

The change in the aquifer hydrological stage can be due to natural and anthropogenic causes and is related to the variation in the hydraulic heads, which may be associated with a significant variation in the groundwater level and storage in unconfined aquifers.

On a regional or global spatial scale, the hydrological crustal deformation due to varying groundwater masses can be explained by the so-called loading model (WAHR *et alii*, 2013; LAROCHELLE *et alii*, 2022; WHITE *et alii*, 2002). Based on this model, when a mass loads (or unloads) the Earth's surface or the underground, the crust

undergoes deformation so that any nearby site moves downward (or upward) and converges (or diverges) toward the load.

This deformational mechanism is juxtaposed against an additional deformational mechanism related to the variations in the piezometric levels (HAMMOND *et alii*, 2016). In particular, soil subsidence and uplift associated with groundwater drawdown and recharge characterize porous alluvial aquifers (BAWDEN *et alii*, 2001; KING *et alii*, 2007). In this case, deformations are due to changes in the effective stresses caused by pore water pressure variations associated with water table rising and lowering (WANG, 2000; WISELY & SCHMIDT, 2010; RIEL *et alii*, 2018).

Some karst massifs of the Apennine chain (Italy) are monitored by one or more permanent GNSS stations, providing continuous ground motion records. Recent GNSS studies have shown that also karst massifs undergo hydrological deformation (DEVOTI *et alii*, 2015; SILVERII *et alii*, 2016; D'AGOSTINO *et alii*, 2018; SILVERII *et alii*, 2019; LEONE *et alii*, 2023a). In particular, a hydrological component affects horizontal ground displacements measured at single GNSS stations. On the other hand, the hydrological patterns are often less evident in the vertical component, and data from several GNSS stations could be required to reveal the hydrological component.

Previous studies have applied a specific modeling approach to explain the observed hydrological deformation of karst massif, attributing this phenomenon to the widening and closing of water-filled fractures due to the continuous hydraulic head fluctuations associated with the aquifer recharge and discharge processes, respectively. Thus, the overall deformation would be the cumulated effect of several distinct sources, and the latter can be approximated as a single equivalent tensile fracture in an elastic half-space (DEVOTI *et alii*, 2018; SERPELLONI *et alii*, 2018; BRAITENBERG *et alii*, 2019). The main limitation of this model is that it attributes karst massif deformation exclusively to the hydrodynamic of major fractures, neglecting the role of the pore water pressure. Indeed, a karst aquifer is a triple porosity medium in which groundwater fills (i) fractures, (ii) large voids and conduits, and (iii) pores and fissures of the rock matrix as well (FORD & WILLIAMS, 2007). The main groundwater reservoir is stored in the aquifer saturated zone comprising the karst network and the low-permeability matrix with a high storage capacity, and water exchanges occur between the karst network and the matrix (WHITE, 2003; FIORILLO *et alii*, 2022).

The pore fluid pressure is a fundamental component of the in-situ stress state (BARTON & ZOBACK, 1988; ENGELDER & FISCHER, 1994; AMADEI & STEPHANSSON, 1997; ZOBACK, 2007). In the specific case of karst aquifers, the variation in the groundwater level should lead to a change in the stress state acting in a wide rock volume (aquifer saturate zone, primarily, and epiphreatic zone, secondarily) according to Terzaghi's effective stress principle (TERZAGHI, 1923, 1936; SKEMPTON, 1961a). As

wide water table oscillations characterize karst aquifers, pore water pressure variations can be up to thousands of KPa, and significant changes in the stress state are expected to occur.

This paper focuses on the Matese karst massif (southern Apennine) and discusses the relationships between karst aquifer hydrological variability and crustal deformation detected through the analysis of GNSS data. Time series analysis methods were applied to highlight the presence of hydrological components in geodetic time series. GNSS observations were integrated with InSAR data, the latter provided by the European Ground Motion Service (EGMS).

The study also illustrates new equations explaining such relationships, which are primarily based on Skempton's generalization of Terzaghi's effective stress principle (SKEMPTON, 1961a) and classical linear elasticity. The study highlights that the pore water pressure variation associated with the water table rising and lowering is the primary driver of the observed hydrological deformation, which can be compared to the thermal

expansion of solids. Under unconstrained conditions, the karst aquifer is free to expand laterally, and the hydrological strain depends on the overall elastic properties of the karst rock mass and the coefficient of earth pressure at rest,  $K_0$ . Under constrained conditions, an elastic aquitard laterally bounds the karst aquifer, and the hydrological strain also depends on the elastic properties and dimensions of the aquitard. The resulting strain is thus a fraction of the unconstrained hydrological strain. The hydrological horizontal ground displacements measured by GNSS stations at the surface result from the hydrological deformation accumulated across the aquifer and depend on the location of the stations.

**STUDY AREA**

The Matese massif (Fig. 1) is a NW-SE oriented carbonate horst located at the boundary between central and southern Apennines (Italy), surrounded by the extensional tectonic basins of the Volturno River Plain and Bojano Plain.

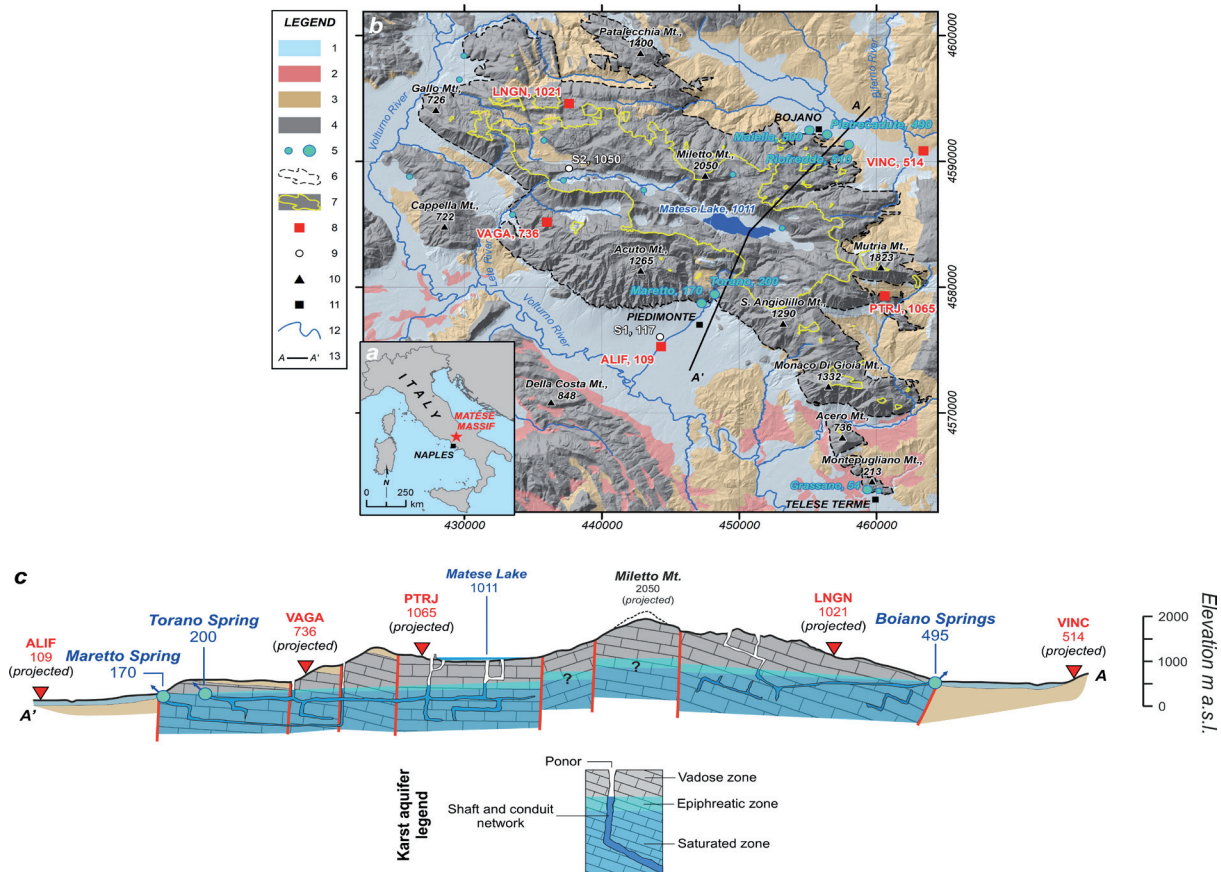


Fig. 1 - Map of Italy (a; coordinate system: UTM WGS84 33N) and geological sketch of the Matese karst area (b). LEGEND: 1) slope breccias and debris, alluvial, lacustrine and travertine deposits (Quaternary); 2) pyroclastic deposits (Quaternary); 3) argillaceous complexes and flysch sequences (Paleogene- Miocene); 4) dolomite-limestone sequences (Triassic-Miocene); 5) karst spring and major karst basal spring (with elevation); 6) karst massif boundary; 7) internal runoff area; (8) GNSS station; 9) meteorological station; 10) mountain peak (with elevation); 11) main village; 12) major river; 13) section trace. Hydrogeological cross-section (c) along the trace A-A', showing the karst aquifer (vadose, epiphreatic, and saturated zone) dissected by faults (red lines) and bounded by aquitards made of argillaceous complexes and flysch sequences (from LEONE et alii, 2023b)

The Matese massif constitutes a wide karst system (540 km<sup>2</sup>), with topographic elevations between approximately 50 and 2,050 m a.s.l. and more than 50% of the surface above 900 m a.s.l. It is made of a highly permeable and thick limestone and limestone-dolomite sequence (2,500-3,000 m) of Triassic-Miocene age, dissected by faults having prevalent NW-SE and NE-SW trends.

Low-permeability synorogenic Miocene silico-clastic deposits made of sandstone, marls, and clays of Tortonian-Messinian age crop out along the edges of the massif and are locally preserved within the tectonic depressions. Along the northern-easter side, the carbonate sequence overlies the Miocene deposits by thrust and compressional faults. Low-permeability pelagic deposits, primarily clay and marls of lower Oligocene-lower Miocene, also crop out in the area. Normal faults bound the massif along the southern and western sides, dividing it from the Volturno River Plain. Medium to high-permeability Quaternary deposits cover the carbonate slopes and fill the alluvial plains and tectono-karstic depressions, including endorheic basins. Quaternary deposits are made of different terrains, including slope breccias and debris, alluvial fan deposits, glacial deposits, pyroclastic deposits, residual soils, travertine, and fluvial and lacustrine deposits.

The climate is Mediterranean. Precipitation mainly occurs during the cold season. The wettest and driest months are November and July, respectively. Precipitation can be snowy during winter at high elevations (> 1000 m a.s.l.). The temperature and potential evapotranspiration time patterns are almost opposite to precipitation, with a maximum occurring in July-August and a minimum in December-February.

Endorheic areas occupy the summit sectors of the massif and represent the catchment of dolines and ponors (PAGNOZZI *et alii*, 2019). Therefore, the aquifer recharge occurs in a diffuse way (infiltration is distributed over a surface) and in a concentrated way (infiltration is concentrated at ponors and dolines; JEANNIN 2001). The extension of endorheic areas ranges from a few up to several square kilometers (LEONE *et alii*, 2022), and the major ones are associated with the tectono-karstic poljes of the Matese Lake (43 km<sup>2</sup>), Letino Lake (22 km<sup>2</sup>), and Gallo Lake (14 km<sup>2</sup>). Another major endorheic area is that of the Inferno Valley (21 km<sup>2</sup>), in the eastern sector of the massif. Before reaching the saturated zone, water percolates through the thick aquifer vadose zone, locally characterized by a width up to hundreds or thousands of meters.

The Matese massif feeds three main basal spring groups. (i) The Torano (201 m a.s.l.) and Maretto springs (170 m a.s.l.) are located along the southern slope of the massif and have a mean discharge of 2.0 and 1.0 m<sup>3</sup>/s, respectively. The discharge of these two springs responds to single rainfall events and climate change (FIORILLO *et alii*, 2021). As observed in other karst areas of the southern Apennine (LEONE *et alii*, 2021), a decreasing trend has characterized karst spring discharge since 1960, and hydrological droughts have stricken the aquifer in the last 30 years. (ii) The

Grassano-Telese springs (50-55 m a.s.l.) are located in the southernmost sector of the massif and are made by large fresh and sulfurous thermal springs closely located, with a mean discharge of 4.5 and 0.2 m<sup>3</sup>/s, respectively (LEONE *et alii*, 2019). The Grassano springs, in particular, are located in the most depressed sector of Matese massif and are fed by an upwelling groundwater flow (FIORILLO *et alii*, 2019). (iii) The Bojano springs are located along the northern side of the massif and have an overall mean discharge of 2.80 m<sup>3</sup>/s (FIORILLO & GUADAGNO, 2012).

## HYDROLOGICAL COMPONENT IN GROUND DISPLACEMENT TIME SERIES

This study uses time series analysis methods to investigate the presence of hydrological components in GNSS and InSAR ground motion measurements. These hydrological components should primarily be associated with changes in the karst aquifer hydrological stage, represented by changes in the groundwater levels and spring discharge.

### *Hydrological and ground displacement data*

The discharge of Torano and Maretto karst springs has been monitored since the 1960s; the time series of these two springs were employed in this study to describe the temporal variability of the aquifer hydrological conditions.

Ground displacements along the north-south, east-west, and vertical directions (north, east, and vertical components, respectively) have been recorded since 2005 by five permanent GNSS stations. As shown by Fig. 1, the VAGA (Valle Agricola), LNGN (Longano), and PTRJ (Pietraraja) stations are placed on the karst massif, while the VINC (Vinchiaturro) and ALIF (Alife) stations are placed outside the karst rock outcrop. Analyses carried out in this study focused exclusively on the first station group. The presence of a hydrological component in the positioning time series of VINC and ALIF stations was discussed in detail by LEONE *et alii* (2023a).

The European Ground Motion Service (EGMS) also provides ground displacement observations obtained by interferometric processing of SAR images (InSAR-processing) data from Copernicus' Sentinel-1 Earth observation mission. More in detail, the EGMS provides the time series of the millimeter-scale position of natural and anthropogenic ground features, such as bare rocks and structures, that happen to reflect back the satellite's radar pulse. Three levels of InSAR products are available, and the EGMS Ortho product was used in this study. This product provides the purely vertical and horizontal (E-W) ground motion, resampled to a 100 m grid. The analyzed InSAR time series span from 2016 to 2021, with a regular temporal sampling of six days, even if huge gaps happen in the time series. Figure 2 shows the western Matese massif and InSAR measuring points, the latter represented by pink-colored pixels.

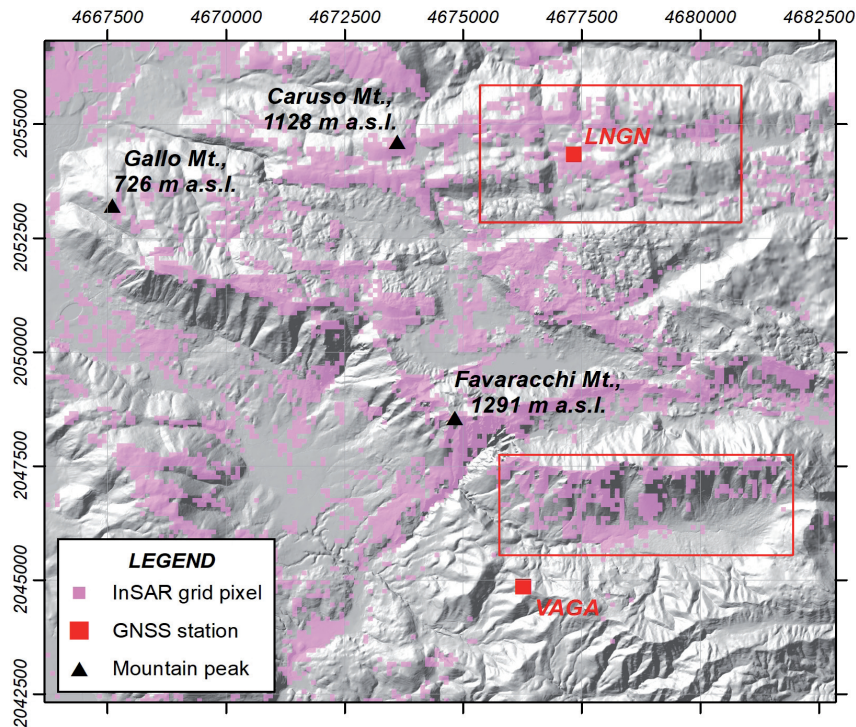


Fig. 2 - Map of the western Matese massif (coordinate system: ETRS 1989 LAEA). Pink squares represent reflecting ground features resampled to a 100 m grid. Displacements plotted in Fig. 4 were obtained by averaging the time series associated with each pixel in the two red rectangles

Ground displacement measurements typically contain linear trends due to regional or local factors (VAN DAM *et alii*, 2001; BAWDEN *et alii*, 2001; WHITE *et alii*, 2022). In many cases, linear trends are due to the regional tectonic motion. However, independently from their nature, linear trends can hide the hydrological components of the ground motion, and for this reason, data are commonly detrended by estimating and removing the best-fit regression line.

*Time series analysis*

Linear trends were estimated and removed from GNSS and InSAR time series to enhance possible seasonal and multi-annual variability due to hydrological factors. Note that detrending also removes the linear hydrological trend component, if any (WHITE *et alii*, 2022).

The resulting time series has a mean equal to 0: increasing displacement values indicate a northward, eastward, and upward motion; otherwise, decreasing displacement values indicate a southward, westward, and downward motion.

Figure 3 shows the spring discharge and GNSS time series from the three measuring sites located on the karst massif. For each GNSS measuring station, the north or the east ground motion component has been plotted, along with the vertical component. The solid red lines represent the 4-year Gaussian moving average,

highlighting the low-frequency time series variability.

The GNSS time series are affected by a seasonal component. Other components associated with low-frequency hydrological variability and groundwater droughts have also been detected in the horizontal ground motion records. In particular, drought years mark the start and end of decreasing spring discharge periods, such as those of 2009-2012 and 2013-2017. As shown by the figure, the main minima and maxima in the horizontal GNSS time series are associated with the main spring discharge minima due to the combined effects of hydrological seasonality and groundwater droughts.

A less clear link with the hydrological conditions of the karst massif characterizes vertical displacements. The vertical motion at the LNGN GNSS station positively correlates to the horizontal one. Unexpectedly, there would be no hydrological component in the time series of vertical displacement measured at the VAGA GNSS station, even if the hydrological control on the horizontal ground motion is the strongest at this site.

Therefore, further analyses were carried out. Figure 4 compares InSAR measurements (detrended vertical displacements) and detrended karst spring discharge. Displacement values represent the average deformation affecting the two areas highlighted in Fig. 2, located north of the VAGA station and around the LNGN station. The vertical deformation detected by InSAR shows a seasonal cycle, and

the maximum subsidence is associated with the 2017 hydrological drought. The figure also shows the 3rd-degree polynomial trend lines, which suggest the presence of a low-frequency hydrological component in the vertical surface deformation.

Differently from GNSS, the InSAR would detect a hydrological vertical deformation affecting the western Matese massif. Generally speaking, a limitation of the GNSS is that it measures the localized ground motion at a given site. A low signal-to-noise ratio often characterizes the time series of the vertical ground displacements, which could obscure the hydrological patterns. The signal-to-noise ratio can be enhanced by stacking the time series acquired at several GNSS sites (SILVERII *et alii*, 2016; SILVERII *et alii*, 2019). However, the main weakness of this technique is due to the scarce density of GNSS stations. The InSAR allows for overcoming this problem as it measures the time variable position of several reflecting ground features. Thus, the ground motion of an area can be obtained by averaging the time series of several measuring points.

## EQUATIONS OF THE HYDROLOGICAL DEFORMATION OF KARST MASSIF

As discussed in the previous study by LEONE *et alii* (2023a), the simultaneous activity of the Matese massif's GNSS stations has revealed that phases of horizontal contraction and dilation are associated with phases of decreasing and increasing spring discharge, respectively. However, the relationships between hydrological variability and vertical motion detected by GNSS measurements were less clear. Using InSAR data, we showed in this study that ground subsidence and uplift in the western Matese massif is associated with decreasing and increasing spring discharge phases, respectively.

Studies have explained the hydrological deformational mechanism of karst massifs as due to the widening and closing of water-filled discontinuities dissecting the rock mass, induced by the increase and decrease in the water pressure into the fractures. Under such a hypothesis, the increases in water pressure would

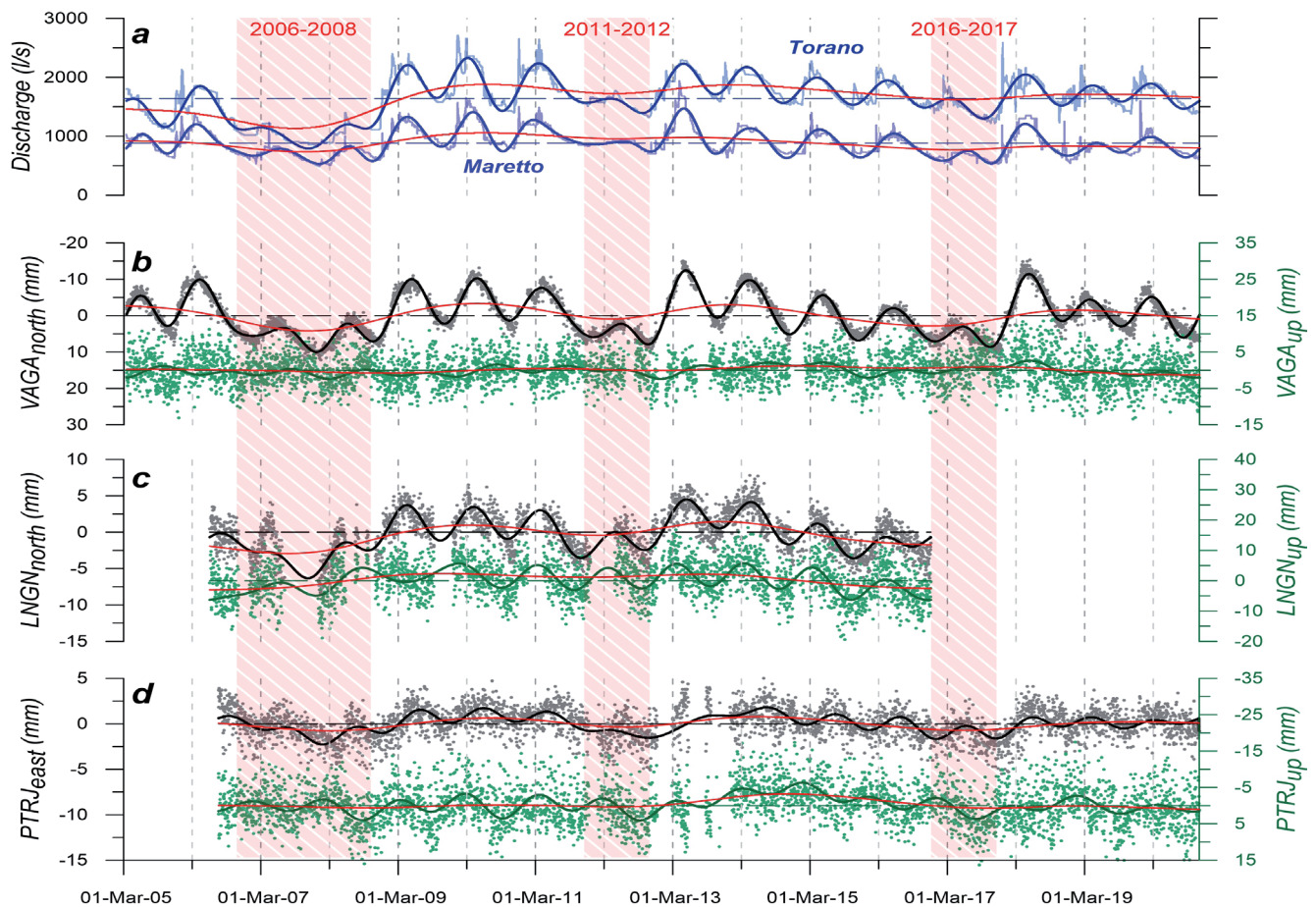


Fig. 3 - Hydrological and ground displacement (GNSS) time series. a) Daily discharge of Torano and Maretto karst springs; red rectangles mark hydrological drought years. b-d) Daily horizontal (gray) and vertical (green) ground displacements measured by GNSS stations located on the karst massif. Smoothed black and green curves were obtained by FFT (Fast Fourier Transform)-based filtering. Dashed lines represent the time series mean. Red lines represent the 4-year Gaussian moving average, highlighting low-frequency variability

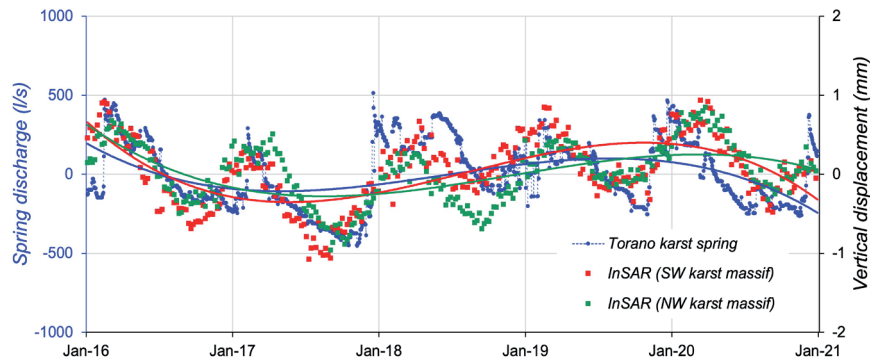


Fig. 4 - Detrended time series of daily spring discharge (Torano spring) and surface deformation. Plotted InSAR data refer to two areas located in the south-western and north-western sectors of the massif (Fig. 2). Time series have mean equal to 0. Smoothed curves represent the 3rd-degree polynomial trend lines

act exclusively in the main fractures causing their widening. The solid portion of the rock mass would undergo no volume changes as this model does not consider pore water pressure variation in the aquifer saturated zone.

However, seasonal oscillations, trends, and droughts in the karst spring discharge primarily reflect the changes in groundwater storage and water table level and, thus, in the pore water pressure in the aquifer saturated zone. A change in pore water pressure leads to a change in the effective stress, which acts exclusively in the solid portion of a rock or soil mass, causing its volumetric deformation as stated by Terzaghi's principle. Therefore, a vast saturated rock volume would undergo deformation in response to water pore pressure changes, even if the network of discontinuities and their characteristics (spacing, width, persistence, filling material, etc.) control the rock mass mechanical behavior.

Recently, LEONE *et alii* (2023b) derived a new set of equations to explain the phenomenon of the hydrological deformation of karst massifs, based on the generalized effective stress formulation proposed by Skempton (SKEMPTON, 1961a) and classical linear elasticity.

Assuming a geostatic stress state and that the rock mass is isotropic and free to expand, the equations relating the horizontal ( $\varepsilon_H$ ) and the vertical ( $\varepsilon_V$ ) strains to the change in the stress state are:

$$\varepsilon_H = -(1/E) [K_0(1 - \nu) - \nu] [\Delta\sigma_V - \alpha \cdot \Delta u] \quad (1)$$

$$\varepsilon_V = -(1/E) [\Delta\sigma_V(1 - 2\nu \cdot K_0)] + (1/E) \alpha \cdot \Delta u [1 - 2\nu \cdot K_0] \quad (2)$$

$E$  and  $\nu$  are Young's modulus and Poisson's ratio,  $\Delta\sigma_V$  is the total vertical stress increment,  $\Delta u$  is the pore water pressure increment, and  $K_0$  is the coefficient of earth pressure at rest. Coefficient  $\alpha$  is known in the literature as effective stress coefficient, poroelastic coefficient, or Biot-Willis's coefficient (WANG, 2000). It is a fundamental parameter in the theory of three-dimensional consolidation of soils published by

Biot in 1941 (BIOT, 1941) even if its physical meaning was explained many years later (BIOT & WILLIS, 1957; GEERTSMA, 1957; SKEMPTON, 1961a; NUR & BYERLEE, 1971).

Assuming no external vertical loads, a change in the water table level causes an increment in  $\Delta\sigma_V$  and  $\Delta u$ :

$$\Delta\sigma_V = n_{eff}(\gamma_w \cdot \Delta h_w) \quad (3)$$

$$\Delta u = (\gamma_w \cdot \Delta h_w) \quad (4)$$

$\Delta\sigma_V$  depends on the effective porosity  $n_{eff}$  which is generally low in karst aquifers and in the range 0.001-0.05 (BONACCI, 1993; DOMENICO & SCHWARTZ, 1998; FORD & WILLIAMS, 2007; WORTHINGTON & FORD, 2009; WORTHINGTON *et alii*, 2012), even if the occurrence of large caves and transportation conduits changes this characteristic locally. Therefore, the total vertical stress increment in equation 3 is negligible compared to the pore water pressure increment.

In the absence of external stresses, the unconstrained horizontal and vertical strains of a saturated karst rock volume under varying pore water pressure are:

$$\varepsilon_H = (\alpha/E) [K_0(1 - \nu) - \nu] \cdot \Delta u \quad (5)$$

$$\varepsilon_V = (\alpha/E) [1 - 2\nu \cdot K_0] \cdot \Delta u \quad (6)$$

Based on equations 5 and 6, the hydrological strain is due to a change in the internal state of stress and depends on the coefficient of earth pressure at rest  $K_0$ . The latter represents the fraction of the effective vertical stress transmitted to the vertical planes of a soil or rock mass and is the fundamental coefficient to properly define the in-situ stress state (SKEMPTON, 1961b). Several theoretical equations were proposed in the literature with the aim of modeling coefficient  $K_0$  (GONZÁLEZ DE VALLEJO, 2006), even if its determination by in-situ and laboratory measurements or its theoretical estimation

is far from simple, also due to the difficulty in separating and modeling the various components of the in-situ stress (ENGELDER & SBAR, 1984; ENGELDER, 1993; ZANG & STEPHANSSON, 2010).

If  $K_0 \neq 1$ , the effective horizontal and vertical stresses do not vary at the same rate when water pore pressure changes. Thus, the unconstrained hydrological strain is not equal in the horizontal and vertical directions, even though the material has isotropic elastic properties.

The stress-strain equations presented here explain the hydrological deformation of the karst massif in its generality. Given the hydraulic features of karst aquifers, the hydrological deformation must involve a wide rock volume placed below the water table and cannot be attributed exclusively to the widening/closing of water-filled fractures, as discussed by many previous studies.

A detailed modeling of the karst massif hydrological deformation should account for the rock mass anisotropy, affecting the orientation of the stress field and rock mechanical properties of the rock (HERGET, 1993; PAN *et alii*, 1995; AMADEI & STEPHANSSON, 1997), and the complex hydrodynamic. Normally, groundwater level changes across the aquifer system are not uniform and synchronous and the pressure changes in the matrix may lag pressure changes in channels (WORTHINGTON & SOLEY, 2017). Groundwater levels react faster in the karst network than in pores and fissures after a recharge event, and time is needed until the groundwater level is established for the entire karst massif (BONACCI, 1993).

Equations 1 and 2 highlight that all aquifers undergo hydrological deformation in response to the variation in effective stress state in the aquifer saturated zone. The latter is due to a positive or negative increment in the pore

water pressure caused by the rising or lowering of the water table, respectively. The magnitude of the hydrologically induced ground displacements depends on the deformation accumulated across the aquifer saturated zone, as illustrated by the theoretical example in Fig. 5. For graphical purposes, the thickness of the saturated zone has been assumed 1/10 of its width. It can be seen that the horizontal displacement amplitude increases moving toward the aquifer edges, while the vertical displacement amplitude increases upward. In Fig. 5, the aquifer is isotropic and laterally unconstrained, and the pore water pressure increment is uniform in space.

As shown by the figure, the dimensions of the saturated zone control the magnitude of the hydrological deformation. Since the width of karst aquifer saturated zone is normally much greater than its thickness, the amplitude of the horizontal ground displacements is expected to be greater than the amplitude of the vertical ones. A  $K_0 < 1$  and high Poisson's ratio favor the vertical strain rather than the horizontal one.

If the aquifer is laterally constrained by an elastic aquitard, the hydrological horizontal elongation  $\epsilon_H^*$  is a fraction of the unconstrained strain  $\epsilon_H$ :

$$\epsilon_H^*/\epsilon_H < 1 \tag{7}$$

Assuming that pore water pressure varies exclusively in the karst aquifer, the  $\epsilon_H^*/\epsilon_H$  ratio is given by the following equation (Fig. 6)

$$\epsilon_H^*/\epsilon_H = 1 / (1 + E_S/E_K \cdot L_K/L_S) \tag{8}$$

where  $L_K$  is the initial length of the karst aquifer (having Young's modulus  $E_K$ ), and  $L_S$  is the initial length of the

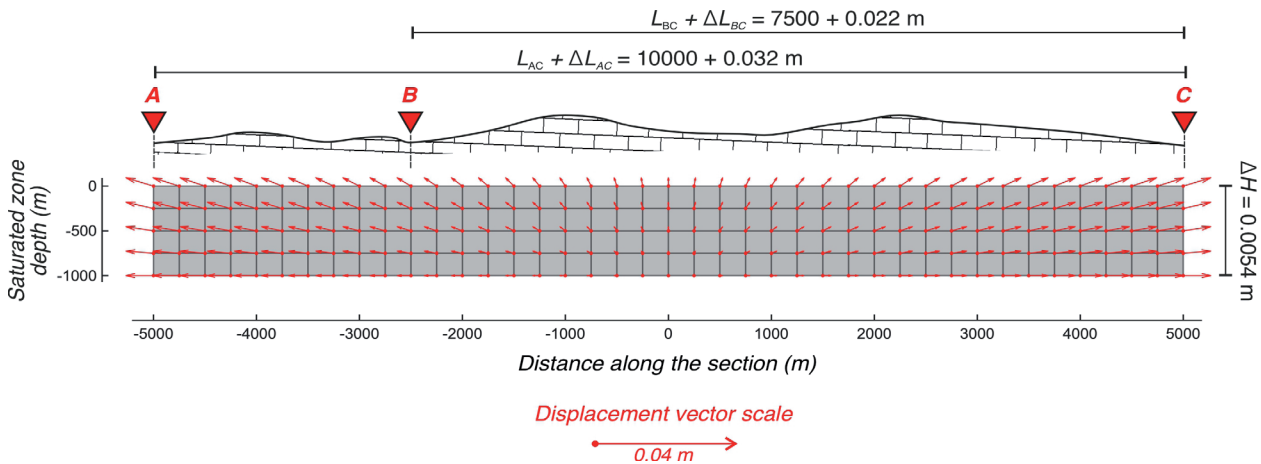


Fig. 5 - Karst aquifer deformation due to a uniform water table increase of 50 m. The aquifer saturated zone is 10000 wide and 1000 m thick and lies on a rigid substratum. Vectors represent the displacement of each grid node, calculated assuming unconstrained conditions, a rock mass with isotropic elastic properties ( $E = 40$  GPa,  $\nu = 0.025$ ,  $\alpha = 0.73$ ), and a coefficient of earth pressure at rest  $K_0 = 0.8$ . The horizontal distance between hypothetical GNSS stations (A, B, and C) increases by an amount  $\Delta L = \epsilon_H \cdot L_{AC}$ , where  $\epsilon_H$  is the horizontal strain and  $L_{AC}$  and  $L_{BC}$  are the initial distances between the stations. The vertical displacement component is  $\Delta H = \epsilon_v \cdot H$ , where  $\epsilon_v$  is the vertical strain, and  $H$  is the saturated zone thickness

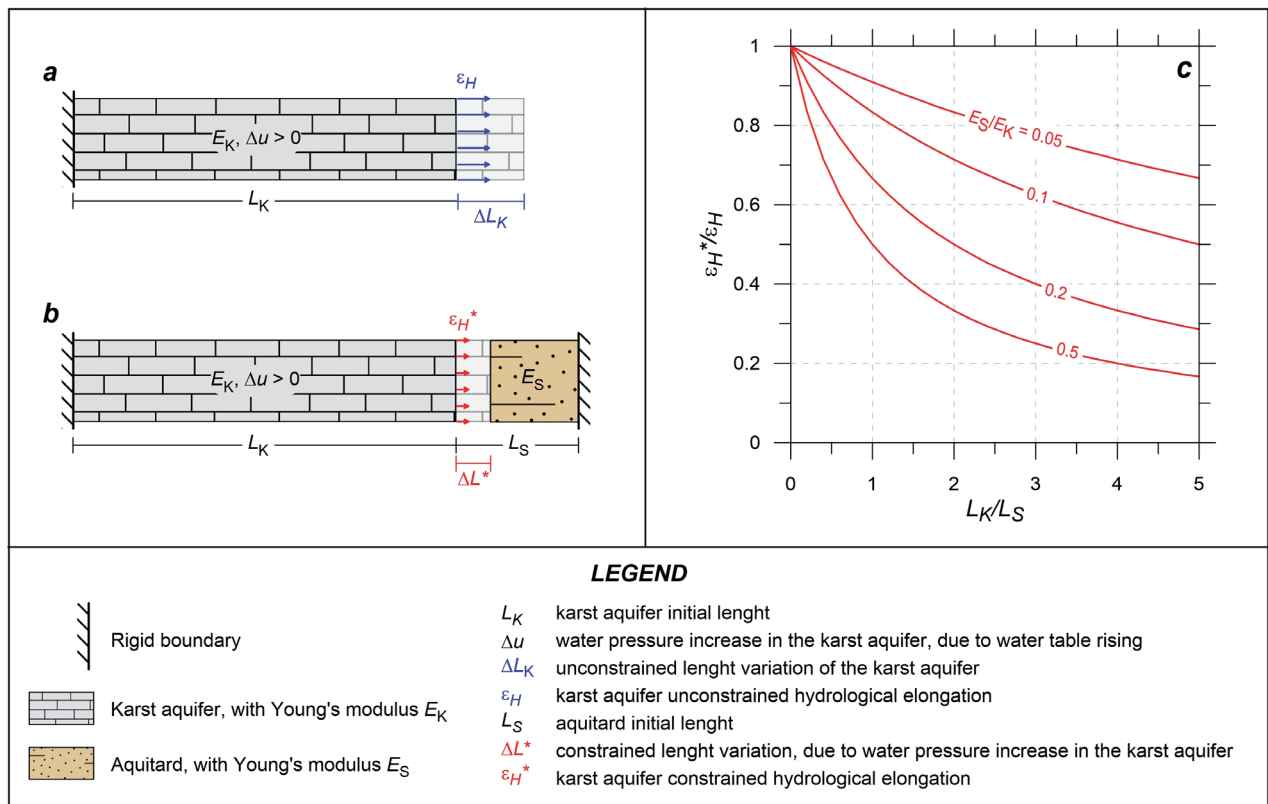


Fig. 6 - Unconstrained hydrological expansion of a karst aquifer due to an increase in the pore water pressure (a); the karst aquifer laterally expands by an amount  $\Delta L_K$ . Constrained hydrological expansion of a karst aquifer bounded on the right by an elastic aquitard (b); the karst aquifer laterally expands by an amount  $\Delta L^* < \Delta L_K$ . Constrained to unconstrained hydrological elongation ratio,  $\varepsilon_H^*/\varepsilon_H$ , as a function of the  $L_K/L_S$  ratio and for different values of the  $E_S/E_K$  ratio (c); from LEONE et alii, 2023b)

aquitard (having Young's modulus  $E_S$ ). The  $\varepsilon_H^*/\varepsilon_H$  ratio depends on the  $E_K/E_S$  and  $L_S/L_K$  ratios: when  $E_K \gg E_S$  and  $L_K \ll L_S$ , the role of the laterally constraining aquitard becomes negligible and the constrained hydrological elongation  $\varepsilon_H^*$  tends to unconstrained one ( $\varepsilon_H$ ).

## CONCLUSIONS

In this study we analyzed GNSS, InSAR, and karst spring discharge data to highlight ground motion components associated with variations in the hydrological stage of the Matese aquifer. We found seasonal oscillations in ground displacement data, but it must be stressed that this does not necessarily mean that the hydrological variability induces surface deformation, as seasonal cycles characterize a number of natural processes. However, we detected low-frequency oscillations in GNSS and InSAR time series which are similar to those affecting the discharge of Torano and Maretto karst springs. In addition, a strong deformational signal associated with below-normal spring discharge conditions was detected in ground displacement time series. More specifically, the main peaks in GNSS time series are related to the 2006-2008, 2011-2012, and 2016-2017 hydrological droughts. The InSAR also

measured a maximum subsidence in the western Matese massif during the summer of 2017. Unfortunately, the limited length of the InSAR records avoids further investigations. The phenomenon of hydrological deformation of karst massifs has been observed all over the Apennine chain and new equations have been discussed in this study to explain it, based on a fundamental principle of soil and rock mechanics, that is, Terzaghi's effective stress principle and elastic theory. In particular, Skempton's formulation of the effective stress was adopted, representing a generalization of Terzaghi's principle applicable to saturated rocks. The equations illustrated in this study provide a physically-based explanation of the observed deformational phenomenon. The latter is related to changes in the overall effective stress state acting in the aquifer saturated zone due to pore water pressure variations induced by water table rising and lowering. The equations found are based on the coefficient of earth pressure at rest,  $K_0$ , which relates the effective vertical stress to the horizontal one. The rock mass deformation occurring at depth causes displacements detectable by GNSS and InSAR, whose amplitude depends on the hydraulic head variations and is the result of the strain cumulated through the aquifer saturated zone. Saturated zone geometry, in turn, and the spatial distribution

of the groundwater masses are further factors controlling the magnitude of aquifer deformation, which would affect the entire saturated rock volume. In particular, karst aquifers of Apennine commonly host groundwater reservoirs occupying large volumes extending for tens or hundreds of square kilometers below the land surface, which should explain the observed amplitude of the horizontal displacements, showing a strong hydrological control.

The hydrological strain (due to a water pressure increment) could be compared to the thermal strain of solids (due to a temperature increment), both caused by a change in the internal stress state of the material. The presence of an aquitard constraining the karst aquifer and having different hydraulic and elastic proprieties hinders the horizontal deformation, and the resulting strain is a fraction of that predicted under unconstrained conditions.

## REFERENCES

- AMADEI B. & STEPHANSSON O. (1997, EDS.) - *Rock stress and its measurement*. Springer, Netherlands, Dordrecht.
- BARTON C.A., ZOBACK M.D. & BURNS K. L. (1988) - *In-situ stress orientation and magnitude at the Fenton Geothermal Site, New Mexico, determined from wellbore breakouts*. *Geophys. Res. Lett.*, **15**(5): 467-470. <https://doi.org/10.1029/GL015i005p00467>
- BAWDEN G.W., THATCHER W., STEIN R.S., HUDNUT K.W. & PELTZER G. (2001) - *Tectonic contraction across Los Angeles after removal of groundwater pumping effects*. *Nature*, **412**(6849): 812-815. <https://doi.org/10.1038/35090558>
- BELL J.W., AMELUNG F., RAMELLI A.R. & BLEWITT G. (2002) - *Land subsidence in Las Vegas, Nevada, 1935–2000: new geodetic data show evolution, revised spatial patterns, and reduced rates*. *Environ. Eng. Geosci.*, **8**(3):155-174. <https://doi.org/10.2113/8.3.155>
- BIOT M.A. (1941) - *General theory of three-dimensional consolidation*. *J. Appl. Phys.*, **12**(2): 155-164. <https://doi.org/10.1063/1.1712886>
- BIOT M.A. & WILLIS D.G. (1957) - *The elastic coefficients of the theory of consolidation*. *J. Appl. Mech.*, **24**(4): 594-601. <https://doi.org/10.1115/1.4011606>
- BONACCI O. (1993) - *Karst springs hydrographs as indicators of karst aquifers*. *Hydrological Sciences -Journal- des Sciences Hydrologiques*, **38**: 51-62. <https://doi.org/10.1080/02626669309492639>
- BRAITENBERG C., PIVETTA T., BARBOLLA D.F., GABROVŠEK F., DEVOTI R. & NAGY I. (2019) - *Terrain uplift due to natural hydrologic overpressure in karstic conduits*. *Sci. Rep.*, **9**(1). <https://doi.org/10.1038/s41598-019-38814-1>
- D'AGOSTINO N., SILVERII F., AMOROSO O., CONVERTITO V., FIORILLO F., VENTAFRIDDA G. & ZOLLO A. (2018) - *Crustal deformation and seismicity modulated by groundwater recharge of Karst aquifers*. *Geophys. Res. Lett.*, **45**(22): 253-262. <https://doi.org/10.1029/2018GL079794>
- DEVOTI R., RIGUZZI F., CINTI F.R. & VENTURA G. (2018) - *Long-term strain oscillations related to the hydrological interaction between aquifers in intra-mountain basins: a case study from Apennines chain (Italy)*. *Earth Planet. Sci. Lett.*, **501**: 1-12. <https://doi.org/10.1016/j.epsl.2018.08.014>
- DEVOTI R., ZULIANI D., BRAITENBERG C., FABRIS P. & GRILLO B. (2015) - *Hydrologically induced slope deformations detected by GPS and clinometric surveys in the Cansiglio Plateau, southern Alps*. *Earth Planet. Sci. Lett.*, **419**: 134-142. <https://doi.org/10.1016/j.epsl.2015.03.023>
- DOMENICO P.A. & SCHWARTZ F.W. (1998, EDS.) - *Physical and chemical hydrogeology*. Wiley, New York.
- ENGELDER T. (1993, EDS.) - *Stress regimes in the lithosphere*. Princeton University Press, Princeton, NJ, Course Book.
- ENGELDER T. & FISCHER M.P. (1994) - *Influence of poroelastic behavior on the magnitude of minimum horizontal stress,  $S_h$ , in overpressured parts of sedimentary basins*. *Geology*, **22**: 949-952.
- ENGELDER T. & SBAR M.L. (1984) - *Near-Surface in Situ Stresses: Introduction*. *J. Geophys. Res.*, **89**(B11): 9321-9322.
- FIORILLO F. & GUADAGNO F.M. (2012) - *Long karst spring discharge time series and droughts occurrence in Southern Italy*. *Environ. Earth. Sci.*, **65**(8): 2273-2283. <https://doi.org/10.1007/s12665-011-1495-9>
- FIORILLO F., ESPOSITO L., LEONE G. & PAGNOZZI M. (2022) - *The Relationship between the Darcy and Poiseuille Laws*. *Water*, **14**. <https://doi.org/10.3390/w14020179>
- FIORILLO F., LEONE G., PAGNOZZI M., CATANI V., TESTA G. & ESPOSITO L. (2019) - *The upwelling groundwater flow in the Karst area of Grassano-Telesse springs (Southern Italy)*. *Water*, **11**(5). <https://doi.org/10.3390/w11050872>
- FIORILLO F., LEONE G., PAGNOZZI M. & ESPOSITO L. (2021) - *Long-term trends in karst spring discharge and relation to climate factors and changes*. *Hydrogeol. J.*, **29**(1): 347-377. <https://doi.org/10.1007/s10040-020-02265-0>
- FORD D. & WILLIAMS P. (2007, EDS.) - *Karst hydrogeology and geomorphology*. John Wiley & Sons Ltd, West Sussex, England
- GEERTSMA J. (1957) - *The effect of fluid pressure decline on volumetric changes of porous rocks*. *Trans AIME*, **210**(01): 331-340. <https://doi.org/10.2118/728-G>
- GONZÁLEZ DE VALLEJO L.I. (2006) - *Geingegneria*. Pearson Education Italia, Milan, Italy.
- HAMMOND W.C., BLEWITT G. & KREEMER C. (2016) - *GPS Imaging of vertical land motion in California and Nevada: Implications for Sierra Nevada uplift*. *J. Geophys. Res. Solid Earth*, **121**(10): 7681-7703. <https://doi.org/10.1002/2016JB013458>
- HERGET G. (1993) - *Rock stresses and rock stress monitoring in Canada*. In: *Rock Testing and Site Characterization*. Elsevier.
- JEANNIN P.Y. (2001) - *Modeling flow in phreatic and epiphreatic karst conduits in the Hoffloch cave (Muotatal, Switzerland)*. *Water Resources Research*, **37**(2): 191-200.
- KING N.E., ARGUS D., LANGBEIN J., AGNEW D.C., BAWDEN G., DOLLAR R.S., LIU Z., GALLOWAY D., REICHARD E., YONG A., WEBB F.H., BOCK Y., STARK K. & BARSEGHIAN D. (2007) - *Space geodetic observation of expansion of the San Gabriel Valley, California, aquifer system, during heavy rainfall*

- in winter 2004-2005. *J. Geophys. Res.*, **112**(B3). <https://doi.org/10.1029/2006JB004448>
- LAROCHELLE S., CHANARD K., FLEITOUT L., FORTIN J., GUALANDI A., LONGUEVERGNE L., REBISCHUNG P., VIOLETTE S. & AVOUAC J. (2022) - *Understanding the geodetic signature of large aquifer systems: example of the Ozark Plateaus in central United States*. *J. Geophys. Res. Solid Earth*, **127**(3). <https://doi.org/10.1029/2021JB023097>
- LEONE G., CATANI V., PAGNOZZI M., GINOLFI M., TESTA G., ESPOSITO L. & FIORILLO F. (2022) - *Hydrological features of Matese Karst Massif, focused on endorheic areas, dolines and hydroelectric exploitation*. *Journal of Maps*. <https://doi.org/10.1080/17445647.2022.2144497>
- LEONE G., D'AGOSTINO N., ESPOSITO L. & FIORILLO F. (2023a) - *Hydrological deformation of karst aquifers detected by GPS measurements, Matese massif, Italy*. *Environ. Earth Sci.*, **82**(9). <https://doi.org/10.1007/s12665-023-10905-3>
- LEONE G., ESPOSITO L. & FIORILLO F. (2023) - *Terzaghi's Effective Stress Principle and Hydrological Deformation of Karst Aquifers Detected by GNSS Measurements*. *Rock Mechanics and Rock Engineering*. <https://doi.org/10.1007/s00603-023-03688-3>
- LEONE G., PAGNOZZI M., CATANI V., TESTA G., ESPOSITO L. & FIORILLO F. (2019) - *Hydrogeology of the Karst Area of the Grassano and Teleso Springs*. *Acque Sotterranee - Italian Journal of Groundwater*, **415**: 63-68. *Doi*: 10.7343/as-2019-415
- LEONE G., PAGNOZZI M., CATANI V., VENTAFRIDDA G., ESPOSITO L. & FIORILLO F. (2021) - *A hundred years of Caposele spring discharge measurements: trends and statistics for understanding water resource availability under climate change*. *Stoch. Environ. Res. Risk Assess.*, **35**: 345-370. <https://doi.org/10.1007/s00477-020-01908-8>
- NUR A. & BYERLEE J.D. (1971) - *An exact effective stress law for elastic deformation of rock with fluids*. *J. Geophys. Res.*, **76**(26): 6414-6419. <https://doi.org/10.1029/JB076i026p06414>
- PAGNOZZI M., FIORILLO F., ESPOSITO L. & LEONE G. (2019) - *Hydrological Features of Endorheic Areas in Southern Italy*. *Italian Journal of Engineering Geology and Environment*, **1**: 85-91. *Doi*: 10.4408/IJEGE.2019-01.S-14
- PAN E., AMADEI B. & SAVAGE W.Z. (1995) - *Gravitational and tectonic stresses in anisotropic rock with irregular topography*. *Int. J. Rock Mech. Min. Sci. Geomech. Abstr.*, **32**(3): 201-214. [https://doi.org/10.1016/0148-9062\(94\)00046-6](https://doi.org/10.1016/0148-9062(94)00046-6)
- RIEL B., SIMONS M., PONTI D., AGRAM P. & JOLIVET R. (2018) - *Quantifying ground deformation in the Los Angeles and Santa Ana coastal basins due to groundwater withdrawal*. *Water Resour. Res.*, **54**(5): 3557-3582. <https://doi.org/10.1029/2017WR021978>
- SERPELLONI E., PINTORI F., GUALANDI A., SCOCIMARRO E., CAVALIERE A., ANDERLINI L., BELARDINELLI M.E. & TODESCO M. (2018) - *Hydrologically induced Karst deformation: insights from GPS measurements in the Adria-Eurasia plate boundary zone*. *J. Geophys. Res. Solid Earth*, **123**(5): 4413-4430. <https://doi.org/10.1002/2017JB015252>
- SILVERII F., D'AGOSTINO N., MÉTOIS M., FIORILLO F. & VENTAFRIDDA G. (2016) - *Transient deformation of karst aquifers due to seasonal and multiyear groundwater variations observed by GPS in southern Apennines (Italy)*. *J. Geophys. Res. Solid Earth*, **121**(11): 8315-8337. <https://doi.org/10.1016/j.epsl.2018.10.019>
- SILVERII F., D'AGOSTINO N., BORSA A.A., CALCATERRA S., GAMBINO P., GIULIANI R. & MATTONE M. (2019) - *Transient crustal deformation from karst aquifers hydrology in the Apennines (Italy)*. *Earth Planet Sci. Lett.*, **506**: 23-37. <https://doi.org/10.1002/2016JB013361>
- SKEMPTON A.W. (1961a) - *Effective Stress in Soils, Concrete and Rocks*. In: *Pore Pressure and Suction in Soils*. Butterworths, London, England.
- SKEMPTON A.W. (1961b) - *Horizontal Stresses in an Over-Consolidated Eocene Clay*. In: *Proc. 5th Int. Conf. Soil Mech.* Dunod, Paris, France: 351-357.
- TERZAGHI K. (1923) - *Die Berechnung der Durchlässigkeitsziffer des Tonen aus Dem Verlauf der Hydrodynamischen Spannungserscheinungen Akademie der Wissenschaften in Wien. Math. Nat. Schaffiliche.*, **132**: 105-124.
- TERZAGHI K. (1936) - *The shearing resistance of saturated soils. Proceedings in 1st International Conference on Soil Mechanics and Foundation Engineering*. Massasuchets, United States, Cambridge: 54-56.

Received January 2024 - Accepted March 2024